# Diffracted Transition Radiation of a Relativistic Electron in a Three-Layer Structure

## S. V. Blazhevich, R. A. Zagorodnyuk, and A. V. Noskov

*Belgorod State National Research University, Belgorod, 308015 Russia*

*e-mail: noskovbupk@mail.ru*

**Abstract**—We develop a theory of coherent X-ray radiation of a relativistic electron crossing a three-layer structure consisting of two amorphous layers and a crystal layer. The particular case when the second amorphous layer is a vacuum is considered. Expressions describing the spectral and angular distributions of coherent radiation in such a structure are derived and analyzed.

## 1. INTRODUCTION

The interest of physicists in the X-ray radiation of various types emitted when electrons pass through structured atomic media has increased in recent years. This interest is due to the possibility of obtaining compact X-ray sources [1] based on the emission mechanism manifested in this case, which are widely used in fundamental and applied studies in solid state physics, microelectronics, medicine, biology, etc. These sources, obtained on the basis of synchrotron radiation generated in electron storage rings with an energy of about 1 GeV, are bulky and costly devices. For this reason, the exploration of possibilities of obtaining more compact alternative X-ray sources is topical.

It should be noted that compact X-ray sources being developed on the basis of transition radiation from relativistic electrons in amorphous media [2, 3], parametric X-ray radiation emitted by relativistic electrons in crystals [4, 5], as well as radiation emitted upon channeling of electrons in crystals [6], were considered most suitable for applications [7]. However, calculations and experimental data revealed that all these sources are not very effective because of the low intensities of the beams of emitted X-ray photons even for strong electron currents. Thus, the search for mechanisms of generation of X-rays by relativistic electrons in structured media, which would increase the intensity of emitted X-rays, remains topical.

One of the most promising emission mechanisms for this purpose is the diffracted transition radiation (DTR) of relativistic electrons in crystals [8–11], emerging as a result of the dynamic diffraction of photons of transition radiation generated at the front face of the crystal from atomic planes of a crystal target. DTR is the effect of the dynamic diffraction of transition radiation photons from a system of parallel atomic planes of the crystal, which is manifested in the direction of Bragg scattering in a narrow spectral range; this ensures the advantage of DTR over conventional transition radiation (TR) with a broad spectrum in obtaining a monochromatic X-ray source. Although transition radiation was discovered and studied long ago, it remains an interesting object of investigation for various applications [12–17].

When a relativistic electron crosses a single crystal, its Coulomb field is scattered from the system of parallel atomic planes of the crystal, generating parametric X-ray radiation (PXR) with photons moving in the direction of Bragg scattering together with DTR photons. The theory of coherent X-ray radiation of relativistic electrons in a crystal, which describes the contributions from the DTR and PXR mechanisms using the two-wave approximation of the dynamic theory of diffraction of X-ray waves, was developed in [18–22]. In [18, 19], coherent X-ray radiation was considered in a special case of symmetric reflection, when the reflecting system of atomic planes of the crystal is parallel to the surface of the target (in the case of Bragg scattering geometry) or is perpendicular to it (in the Laue scattering geometry).

In [20–22], a dynamic theory of coherent X-ray radiation of relativistic electrons in a crystal is developed for the general case of asymmetric reflection of the electron field relative to the target surface, when the system of parallel reflecting layers in the target can form an arbitrary angle with the target surface. It is shown that by changing the asymmetry of the reflection of the electron field (i.e., by changing the angle between the target surface and the system of diffracting atomic planes of the crystal), it is possible to substantially increase the spectral–angular density of DTR and PXR.

It should be noted that the contribution to DTR from the crystal target comes only from the transition radiation emerging at its first interface, which rules out an increase in the radiation yield due to a constructive

Fig. 1. Geometry of radiation process and notation for quantities used: $\theta$ and $\theta'$ are emission angles, $\theta_B$ is the Bragg angle (between electron velocity $\mathbf{V}$ and atomic planes), $\delta$ is the angle between the and atomic planes of the crystal layer under investigation, and $\mathbf{k}$ and $\mathbf{k_g}$ are wavevectors of the incident and diffracted photon.

interference of TR waves from different faces. In [23], coherent X-ray radiation of a relativistic electron was considered in a two-layer structure consisting of an amorphous layer and a crystal layer; the possibility of increasing the DTR intensity in this type of structure was demonstrated.

The present study aims at the search for methods of increasing the yield of coherent radiation generated by relativistic electrons in a structured medium. Specifically, we analyze the contribution from the mechanism of transition radiation in a system consisting of a sequence of layers, including several amorphous layers and a single-crystal layer playing the role of the reflector of transition radiation emerging at the interfaces between amorphous layers and at the front face of the crystal layer itself, as well as the role of the emitter for parametric radiation formed on its atomic planes. It would be interesting to consider the interference of radiation waves emerging at different interfaces between the layers and diffracted in the crystal layer in the Bragg direction and PXR in the same direction.

An analysis of the two-layer system "amorphous layer + crystal layer" is interesting for describing the radiation from a single-crystal emitter with a protective layer on the front surface of the crystal or an amorphous layer serving as a substrate (e.g., for a thin crystal). This problem was considered in our previous publication [23]. The case of a three-layer target, considered here, is also of special interest because, on the one hand, it indicates a transition to a multilayer system and, on the other hand, it makes it possible to describe an elementary system consisting of two layers separated by a vacuum layer. The next step in the investigation will be the generalization of results to the case of a multilayer system with an arbitrary number of layers. In this work, the spectral and angular distributions of DTR and PXR in a three-layer structure are

studied in the Laue scattering geometry in the general case of asymmetric reflection.

## 2. RADIATION AMPLITUDE

Let us consider the radiation of a relativistic electron moving rectilinearly with velocity $\mathbf{V}$ across a three-layer structure consisting of two amorphous layers and a crystal layer (Fig. 1) of thickness $c$, $a$, and $b$, respectively. The dielectric susceptibilities of the amorphous media will be denoted by $\chi_c$ and $\chi_a$, while the dielectric susceptibilities of the crystal medium are $\chi_0$ and $\chi_g$.

We consider the propagation of X-ray waves in a crystal medium in a two-wave approximation of the dynamic diffraction theory. In Fig. 1, $\boldsymbol{\mu} = \mathbf{k} - \omega\mathbf{V}/V^2$ is the momentum component of the virtual photon, perpendicular to particle velocity $\mathbf{V}$ ($\mu = \omega\theta/V$, where $\theta \ll 1$ is the angle between vectors $\mathbf{k}$ and $\mathbf{V}$), $\theta_B$ is the Bragg angle, and $\varphi$ is the azimuthal radiation angle measured from the plane formed by velocity vector $\mathbf{V}$ of the electron and reciprocal crystal lattice vector $\mathbf{g}$. The length of vector $\mathbf{g}$ can be expressed in terms of the Bragg angle and Bragg frequency $\omega_B$: $g = 2\omega_B \sin\theta_B/V$; $\theta$ is the angle between vector $\omega\mathbf{V}/V^2$ and wavevector $\mathbf{k}$, and $\theta'$ is the angle between vector $\omega\mathbf{V}/V^2 + \mathbf{g}$ and wavevector $\mathbf{k_g}$ of the diffracted wave.

The emission and diffraction of X-ray waves in the crystal layer in direction $\mathbf{k_g}$ can be described in the two-wave approximation of dynamic diffraction theory [24] analogously to [22, 25]; the same notation as in [23] is used.

The lengths $k_a = \omega\sqrt{1 + \chi_a}$ and $k_c = \omega\sqrt{1 + \chi_c}$ of the wavevector of free photons in amorphous media can be conveniently written in the form

$$k_a = \omega\left(1 + \frac{\chi_0}{2}\right) + \frac{\gamma_0}{\gamma_g}\left(\lambda'_{ga} - \frac{\omega\beta}{2}\right),$$

$$k_c = \omega\left(1 + \frac{\chi_0}{2}\right) + \frac{\gamma_0}{\gamma_g}\left(\lambda'_{gc} - \frac{\omega\beta}{2}\right),$$

$$\tag{1}$$

where

$$\lambda'_{ga} = \lambda^*_g - \frac{\gamma_g}{\gamma_0}\omega\left(\frac{\gamma^{-2} + \theta^2 - \chi_a}{2}\right),$$

$$\lambda'_{gc} = \lambda^*_g - \frac{\gamma_g}{\gamma_0}\omega\left(\frac{\gamma^{-2} + \theta^2 - \chi_c}{2}\right),$$

$$\tag{2a}$$

$$\lambda^*_g = \frac{\omega\beta}{2} + \frac{\gamma_g}{\gamma_0}\lambda^*_0, \quad \lambda^*_0 = \omega\left(\frac{\gamma^{-2} + \theta^2 - \chi_0}{2}\right), \quad \tag{2b}$$

$$\beta = \alpha - \chi_0\left(1 - \frac{\gamma_g}{\gamma_0}\right), \quad \alpha = \frac{1}{\omega^2}(k_g^2 - k^2),$$

$$\gamma_0 = \cos\psi_0, \quad \gamma_g = \cos\psi_g,$$

$\psi_0$ is the angle between wavevector **k** of the incident wave and vector **n** normal to the surface of the crystal wafer, $\psi_g$ is the angle between wavevector $\mathbf{k}_g$ and vector **n** (see Fig. 1), $\gamma$ is the Lorentz factor, $\theta$ and $\theta'$ are the photon radiation angles relative to the velocity of the relativistic electron and the Bragg scattering direction.

Considering the emission process in a three-layer structure analogously to emission in a two-layer structure [23] and using the apparatus of dynamic theory of diffraction of X-ray waves in the crystal wafer described in [22, 25], we obtain the following expression for radiation amplitude $E_g^{(s)\,\mathrm{Rad}}$ in the direction of Bragg scattering, which can be written as the sum of the amplitudes of diffracted transition radiation and parametric X-ray radiation:

$$E_g^{(s)\,\mathrm{Rad}} = E_{\mathrm{DTR}}^{(s)} + E_{\mathrm{PXR}}^{(s)}, \qquad (3a)$$

$$E_{\mathrm{DTR}}^{(s)} = \frac{8\pi^2 i e V\theta P^{(s)}}{\omega}\exp\left\{i\left(\frac{\omega\chi_0}{2}+\lambda_g^*\right)\frac{c+a+b}{\gamma_g}\right\}$$

$$\times \frac{\omega^2\chi_g C^{(s)}}{2\omega\frac{\gamma_0}{\gamma_g}(\lambda_g^{(1)}-\lambda_g^{(2)})}\left(\exp\left\{i\frac{\lambda_g^{(1)}-\lambda_g^*}{\gamma_g}b\right\}\right.$$

$$\left.-\exp\left\{i\frac{\lambda_g^{(2)}-\lambda_g^*}{\gamma_g}b\right\}\right)\left[\left(\frac{1}{\theta^2+\gamma^{-2}-\chi_c}-\frac{1}{\theta^2+\gamma^{-2}}\right)\right.$$

$$\times\exp\left\{-i\frac{\omega c}{2\gamma_0}(\gamma^{-2}+\theta^2-\chi_c)-i\frac{\omega a}{2\gamma_0}(\gamma^{-2}+\theta^2-\chi_a)\right\}$$

$$+\left(\frac{1}{\theta^2+\gamma^{-2}-\chi_a}-\frac{1}{\theta^2+\gamma^{-2}-\chi_c}\right)$$

$$\times\exp\left\{-i\frac{\omega a}{2\gamma_0}(\gamma^{-2}+\theta^2-\chi_a)\right\}$$

$$\left.+\frac{1}{\theta^2+\gamma^{-2}-\chi_0}-\frac{1}{\theta^2+\gamma^{-2}-\chi_a}\right], \qquad (3b)$$

$$E_{\mathrm{PXR}}^{(s)} = \frac{8\pi^2 i e V\theta P^{(s)}}{\omega}\exp\left\{i\left(\frac{\omega\chi_0}{2}+\lambda_g^*\right)\frac{c+a+b}{\gamma_g}\right\}$$

$$\times\frac{\omega^2\chi_g C^{(s)}}{2\omega\frac{\gamma_0}{\gamma_g}(\lambda_g^{(1)}-\lambda_g^{(2)})}\left[\left(\frac{1}{\chi_0-\theta^2-\gamma^{-2}}\right.\right.$$

$$\left.\left.+\frac{\omega}{2\frac{\gamma_0}{\gamma_g}(\lambda_g^*-\lambda_g^{(1)})}\right)\left(\exp\left\{i\frac{\lambda_g^{(1)}-\lambda_g^*}{\gamma_g}b\right\}-1\right)\right.$$
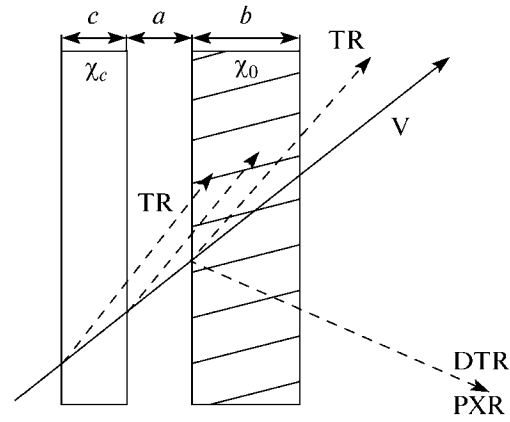


Fig. 2. Process of X-ray generation by relativistic electron in the case where the second amorphous layer is vacuum.

$$\left.-\left(\frac{1}{\chi_0-\theta^2-\gamma^{-2}}+\frac{\omega}{2\frac{\gamma_0}{\gamma_g}(\lambda_g^*-\lambda_g^{(2)})}\right)\right.$$

$$\left.\times\left(\exp\left\{i\frac{\lambda_g^{(2)}-\lambda_g^*}{\gamma_g}b\right\}-1\right)\right]. \qquad (3c)$$

Since PXR is generated only in the crystal layer, expression (3c) for the PXR amplitude coincides with the expression derived in [23]. The properties and spectral—angular characteristics of the PXR in the crystal layer are independent of the characteristics of the amorphous media. Explicit separation of the expressions for the PXR and DTR amplitudes from the three-layer structure considered here makes it possible to analyze the interference of these radiation mechanisms, the results of which depend on the parameters of amorphous layers.

## 3. SPECTRAL—ANGUALAR DENSITY OF RADIATION

Let us consider the radiation of a relativistic electron in the case when the second layer is a vacuum ($\chi_a = 0$) (Fig. 2). To clarify and analyze the effects that are not associated with absorption, we consider a simple case of a thin nonabsorbing target ($\chi_0'' = \chi_c'' = 0$). In this case, we can derive from expression (3b) the relation describing the spectral—angular density of DTR from the three-layer target "amorphous medium—vacuum—crystal" under investigation:

$$\omega\frac{d^2 N_{\mathrm{DTR}}^{(s)}}{d\omega d\Omega} = \frac{e^2}{4\pi^2}\frac{P^{(s)2}}{|\chi_0'|}T_{\mathrm{DTR}}^{(s)}, \qquad (4a)$$

$$T_{\mathrm{DTR}}^{(s)} = T_1^{(s)} + T_2^{(s)} + T_{\mathrm{int}}^{(s)}, \qquad (4b)$$

$$T_1^{(s)} = 4\Omega^2 \left( \frac{1}{\Omega_0^2 + \chi_c'/\chi_0'} - \frac{1}{\Omega_0^2} \right)^2$$

$$\times \sin^2 \left( \frac{B^{(s)}}{2} \frac{c}{b} \frac{1}{\nu^{(s)}} \left( \Omega_0^2 + \frac{\chi_c'}{\chi_0'} \right) \right) R_{\mathrm{DTR}}^{(s)}, \quad (4c)$$

$$T_2^{(s)} = \Omega^2 \left( \frac{1}{\Omega_0^2 + 1} - \frac{1}{\Omega_0^2} \right)^2 R_{\mathrm{DTR}}^{(s)}, \quad (4d)$$

$$T_{\mathrm{int}}^{(s)} = 2\Omega^2 \left( \frac{1}{\Omega_0^2 + 1} - \frac{1}{\Omega_0^2} \right) \left( \frac{1}{\Omega_0^2} - \frac{1}{\Omega_0^2 + \chi_c'/\chi_0'} \right)$$

$$\times \left[ \cos\left( B^{(s)} \frac{a}{b} \frac{1}{\nu^{(s)}} \Omega_0^2 \right) - \cos\left( B^{(s)} \frac{a}{b} \frac{1}{\nu^{(s)}} \Omega_0^2 \right. \right. \quad (4e)$$

$$\left. \left. + B^{(s)} \frac{c}{b} \frac{1}{\nu^{(s)}} \left( \Omega_0^2 + \frac{\chi_c'}{\chi_0'} \right) \right) \right] R_{\mathrm{DTR}}^{(s)},$$

where the expression describing the DTR spectrum has the form

$$R_{\mathrm{DTR}}^{(s)} = \frac{4\varepsilon^2}{\xi^{(s)}(\omega)^2 + \varepsilon} \sin^2\left( \frac{B^{(s)} \sqrt{\xi^{(s)}(\omega)^2 + \varepsilon}}{\varepsilon} \right). \quad (5)$$

In expressions (4) and (5), the following notation is used:

$$\Omega_0^2 = \Omega^2 + \Gamma^2, \quad \Omega = \frac{\theta}{\sqrt{|\chi_0'|}},$$

$$\Gamma = \frac{1}{\gamma\sqrt{|\chi_0'|}}, \quad \nu^{(s)} = \frac{\chi_g' C^{(s)}}{\chi_0'}, \quad (6)$$

$$B^{(s)} = \frac{1}{2\sin(\delta - \theta_{\mathrm{B}})} \frac{b}{L_{\mathrm{ext}}^{(s)}}, \quad \varepsilon = \frac{\sin(\delta + \theta_{\mathrm{B}})}{\sin(\delta - \theta_{\mathrm{B}})}.$$

Functions $T_1^{(s)}$ and $T_2^{(s)}$ describe the DTR spectral–angular densities corresponding to the waves of transition radiation generated in the amorphous layer and at the front face of the crystal layer, and function $T_{\mathrm{int}}^{(s)}$ describes the effect on the total spectral–angular DTR density of interference of these waves.

Parameter $B^{(s)}$ is half the path length of an electron in the crystal layer, which is expressed in terms of the extinction lengths $L_{\mathrm{ext}}^{(s)} = 1/\omega|\chi_g'|C^{(s)}$ of X-ray waves in the crystal.

It should be noted that the resultant expressions have a form convenient for theoretical analysis because these expressions contain important observable characteristics such as the relative thicknesses $c/b$ and $a/b$ of the layers and dielectric susceptibilities $\chi_c'/\chi_0'$ of the amorphous and crystal layers. Instead of

the observation angle $\theta$, we are using the observation angle (parameter $\Omega$) normalized to quantity $\sqrt{|\chi_0'|}$.

The important parameter

$$\varepsilon = \frac{\sin(\delta + \theta_{\mathrm{B}})}{\sin(\delta - \theta_{\mathrm{B}})},$$

in the resultant expressions determines the degree of asymmetry in the reflection of the field in the crystal wafer relative to the target surface.

Constructive interference of waves from different faces of the amorphous layer may substantially increase the DTR spectral–angular density. The condition for constructive interference following from expression (4c) can be written in the form

$$\frac{B^{(s)}}{2} \frac{c}{b} \frac{1}{\nu^{(s)}} \left( \Omega_0^2 + \frac{\chi_c'}{\chi_0'} \right)$$

$$= \frac{\omega c}{4\sin(\delta - \theta_{\mathrm{B}})} (\theta^2 + \gamma^{-2} - \chi_c') = (2n+1)\frac{\pi}{2}, \quad (7a)$$

$$n = 0, 1, 2, \ldots.$$

The spectral–angular DTR density can additionally be increased due to the constructive interference of TR waves from the amorphous layer and from the front face of the crystal layer; the condition for such interference following from expression (4e) has the form

$$B^{(s)} \frac{a}{b} \frac{1}{\nu^{(s)}} \Omega_0^2 = \frac{\omega a}{2\sin(\delta - \theta_{\mathrm{B}})} (\theta^2 + \gamma^{-2})$$

$$= (2m+1)\pi, \quad m = 0, 1, 2, \ldots. \quad (7b)$$

It can be shown that for $|\chi_0'| > |\chi_c'|$, interference term $T_{\mathrm{int}}^{(s)}$ may exceed the contribution of each TR to the total DTR yield. In the particular case where $\chi_0' = \chi_c'$, expressions (4) under conditions (7a) and (7b) lead to the expression

$$\omega \frac{d^2 N_{\mathrm{DTR}}^{(s)}}{d\omega d\Omega} = 9 \frac{e^2}{4\pi^2} P^{(s)2} \theta^2$$

$$\times \left( \frac{1}{\theta^2 + \gamma^{-2} - \chi_0'} - \frac{1}{\theta^2 + \gamma^{-2}} \right)^2 R_{\mathrm{DTR}}^{(s)}, \quad (8)$$

which shows that the spectral–angular DTR density from the three-layer target under investigation under these conditions is nine times greater then the spectral–angular DTR density from the single-crystal layer.

Diffracted transition radiation of a relativistic electron from the three-layer structure under investigation is accompanied by parametric X-ray radiation generated in the crystal layer. The interference of these radiation mechanisms can considerably

affect the spectral–angular density of the total radiation. Using expression (3c), we obtain the following relation describing the spectral–angular PXR density:

$$\omega \frac{d^2 N_{PXR}^{(s)}}{d\omega d\Omega} = \frac{e^2}{4\pi^2} \frac{P^{(s)^2}}{|\chi_0'|} T_{PXR}^{(s)}, \qquad (9a)$$

$$T_{PXR}^{(s)} = \frac{\Omega^2}{(\Omega^2 + \Gamma^2 + 1)^2} R_{PXR}^{(s)}, \qquad (9b)$$

$$R_{PXR}^{(s)} = 4\left(1 - \frac{\xi}{\sqrt{\xi^2 + \varepsilon}}\right)^2$$

$$\times \frac{\sin^2\left(\frac{B^{(s)}}{2}\left(\sigma^{(s)} + \frac{\xi - \sqrt{\xi^2 + \varepsilon}}{\varepsilon}\right)\right)}{\left(\sigma^{(s)} + \frac{\xi - \sqrt{\xi^2 + \varepsilon}}{\varepsilon}\right)^2}, \qquad (9c)$$

where

$$\sigma^{(s)} = \frac{1}{v^{(s)}}(\Omega_0^2 + 1).$$

Using expressions (3c) and (3b), we obtain an expression describing the interference of the radiation mechanisms for DTR and PXR in the absence of absorption ($\chi_0'' = \chi_c'' = 0$):

$$\omega \frac{d^2 N_{int}^{(s)}}{d\omega d\Omega} = \frac{e^2}{4\pi^2} \frac{P^{(s)^2}}{|\chi_0'|} T_{PXR,DTR}^{int(s)}, \qquad (10a)$$

where

$$T_{PXR,DTR}^{int(s)} = \frac{\Omega^2}{\Omega_0^2 + 1}\left[\left(\frac{1}{\Omega_0^2 + \frac{\chi_c'}{\chi_0'}} - \frac{1}{\Omega_0^2}\right) R_{int}^{(s)(1)}\right.$$

$$\left. + \left(\frac{1}{\Omega_0^2 + 1} - \frac{1}{\Omega_0^2}\right) R_{int}^{(s)(2)}\right], \qquad (10b)$$

$$R_{int}^{(s)(1)} = -8\varepsilon \frac{\xi^{(s)} - \sqrt{\xi^{(s)^2} + \varepsilon}}{\xi^{(s)^2} + \varepsilon} \sin\left(\frac{B^{(s)}}{2} \frac{c}{b} \frac{1}{v^{(s)}}\left(\Omega_0^2 + \frac{\chi_c'}{\chi_0'}\right)\right)$$

$$\times \sin\left(\frac{B^{(s)}\sqrt{\xi^2 + \varepsilon}}{\varepsilon}\right) \sin\left(\frac{B^{(s)}}{2}\left(\sigma^{(s)} + \frac{\xi - \sqrt{\xi^2 + \varepsilon}}{\varepsilon}\right)\right)$$

$$\times \sin\left(\frac{B^{(s)}}{2}\left(\frac{a}{b}\frac{2}{v^{(s)}}\Omega_0^2 + \frac{c}{b}\frac{1}{v^{(s)}}\left(\Omega_0^2 + \frac{\chi_c'}{\chi_0'}\right)\right.\right.$$

$$\left.\left. + \sigma^{(s)} + \frac{\xi + \sqrt{\xi^2 + \varepsilon}}{\varepsilon}\right)\right), \qquad (11a)$$

$$R_{int}^{(s)(2)} = 4\varepsilon \frac{\xi^{(s)} - \sqrt{\xi^{(s)^2} + \varepsilon}}{\xi^{(s)^2} + \varepsilon} \sin\left(B^{(s)}\frac{\sqrt{\xi^2 + \varepsilon}}{\varepsilon}\right)$$

$$\times \sin\left(\frac{B^{(s)}}{2}\left(\sigma^{(s)} + \frac{\xi - \sqrt{\xi^2 + \varepsilon}}{\varepsilon}\right)\right) \qquad (11b)$$

$$\times \cos\left(\frac{B^{(s)}}{2}\left(\sigma^{(s)} + \frac{\xi + \sqrt{\xi^2 + \varepsilon}}{\varepsilon}\right)\right).$$

Interference spectral functions $R_{int}^{(s)(1)}$ and $R_{int}^{(s)(2)}$ describe the interference of PXR and DTR from the amorphous layer and interference of PXR and DTR from the front face of the crystalline layer, respectively.

The resulting expressions (4), (9), and (10) that describe respectively the spectral–angular DTR and PXR distributions in the three-layer target under investigation and their interference term are obtained for the first time and are the main result of this study. These expressions take into account all interference effects possible in such a structure, as well as the effects associated with asymmetry of reflection (parameter $\varepsilon$). These expressions can be used for analyzing the spectral–angular characteristics of radiation of a relativistic electron in the three-layer structure under investigation depending on parameters of the layers constituting the target and the energy of emitting electrons. The expressions for the angular density of DTR and PXR and for the term describing the interference of these radiation mechanisms can be written in the form

$$\frac{dN_{DTR}^{(s)}}{d\Omega} = \frac{e^2 P^{(s)^2}}{8\pi^2 \sin^2\theta_B}(F_1^{(s)}(\theta) + F_2^{(s)}(\theta) + F_{int}^{(s)}(\theta)), \quad (12a)$$
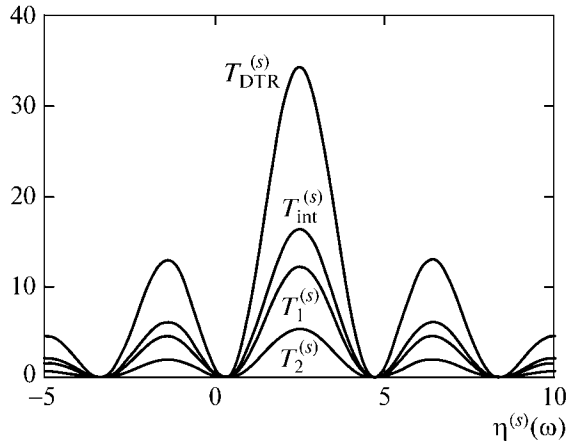
**Fig. 3.** Contributions $T_1^{(s)}$ of TR waves from amorphous wafer, $T_2^{(s)}$ of PXR waves from front boundary of crystal layer, and $T_{int}^{(s)}$ of their interference term to total DTR spectrum $T_{DTR}^{(s)}$. The curves are plotted for constructive interference, $\Omega = \Gamma = 0.5$ (at the angular density peak), $\chi_c'/\chi_0' = 0.5$, $B^{(s)} = 5$, $v^{(s)} = 0.8$, $\varepsilon = 5$, $a/b = 2m + 1$, and $c/b = 0.5(2n + 1)$.

where

$$F_{1,2,int}^{(s)}(\theta) = v^{(s)} \int_{-\infty}^{\infty} T_{1,2,int}^{(s)} d\eta^{(s)}(\omega), \qquad (12b)$$

$$F_{DTR}^{(s)}(\theta) = F_1^{(s)}(\theta) + F_2^{(s)}(\theta) + F_{int}^{(s)}(\theta), \qquad (12c)$$

$$\frac{dN_{PXR}^{(s)}}{d\Omega} = \frac{e^2 P^{(s)^2}}{8\pi^2 \sin^2 \theta_B} F_{PXR}^{(s)}(\theta), \qquad (13a)$$

$$F_{PXR}^{(s)}(\theta) = v^{(s)} \int_{-\infty}^{\infty} T_{PXR}^{(s)} d\eta^{(s)}(\omega), \qquad (13b)$$

$$\frac{dN_{int}^{(s)}}{d\Omega} = \frac{e^2 P^{(s)^2}}{8\pi^2 \sin^2 \theta_B} F_{int}^{(s)}(\theta), \qquad (13c)$$

$$F_{int}^{(s)}(\theta) = v^{(s)} \int_{-\infty}^{\infty} T_{PXR, DTR}^{int(s)} d\eta^{(s)}(\omega). \qquad (13d)$$

## 4. ANALYSIS OF SPECTRAL–ANGULAR PROPERTIES OF RADIATION

We will use the expressions derived in this study for analyzing the spectral–angular properties of radiation. Figure 3 shows curves constructed in accordance with formulas (4c)–(4e) and describing the relative contributions of the waves of transition radiation from the amorphous wafer, TR waves from the front face of the
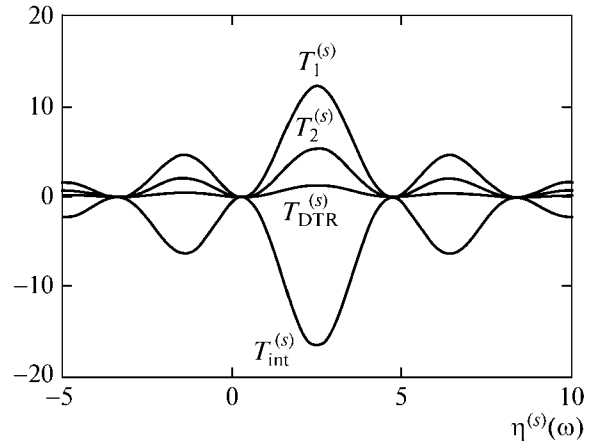


**Fig. 4.** Same as in Fig. 3 for destructive interference of TR waves from amorphous layer and front surface of crystal $(a/b = 2(2m + 1))$.

crystal layer, and their interference term to the total DTR spectrum. The curves in Fig. 3 are plotted for the conditions of the maximum of the angular density $\Omega = \Gamma$ ($\theta = \gamma^{-1}$) of transition radiation and constructive interference for all TR waves (i.e., for the case when both conditions (7) are observed). Constructive interference was attained by selecting the thicknesses of the amorphous layer (parameter $c/b$) and of the vacuum layer (parameter $a/b$), the remaining parameters being fixed. In particular, we fixed parameter $B^{(s)}$ equal to half the electron path length in the crystal layer, expressed in extinction lengths for X-ray waves in the crystal (and, hence, thickness $b$ of the crystal layer itself; see relations (6)). Parameter $v^{(s)}$ (see relations (6)), assuming values from the interval $0 \leq v^{(s)} \leq 1$, determines the degree of reflection of the field from the system of parallel atomic planes in the crystal layer, which depends on the form of the interference of waves
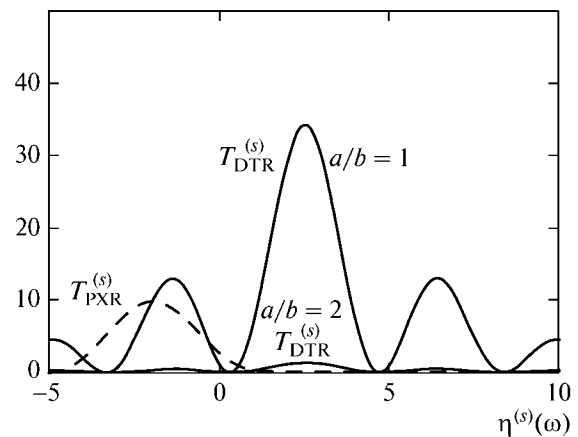


**Fig. 5.** DTR for constructive $(a/b = 2m + 1)$ and destructive $(a/b = 2(2m + 1))$ interference against background of PXR.
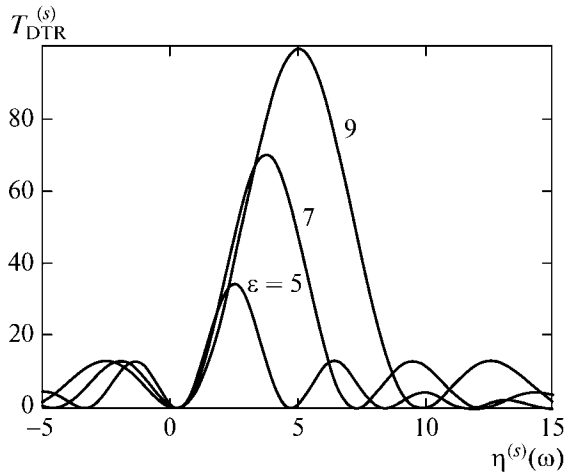
Fig. 6. Effect of asymmetry of reflection in crystal layer on DTR spectrum. Values of parameters are same as in Fig. 3.
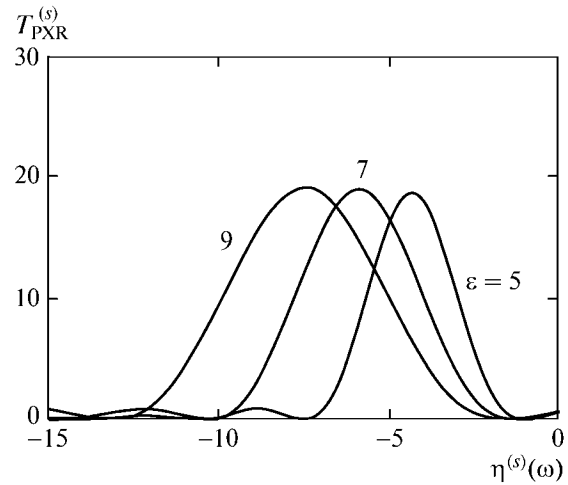


Fig. 7. Effect of asymmetry of reflection of field on PXR spectrum. Values of parameters are same as in Fig. 3. Curves are plotted for $\Gamma = 0.5$, $\Omega = 1$ (at the peak of the PXR angular density), $B^{(s)} = 5$, and $v^{(s)} = 0.8$.

reflected from different planes (constructive interference, $v^{(s)} \approx 1$, or destructive interference, $v^{(s)} \approx 0$).

The curves in Fig. 3 correspond to the case where the term determined by constructive interference of TR from the amorphous layer and the front boundary of the crystal layer in the total DTR spectrum can make a larger contribution to the total DTR spectrum than the contribution from each wave separately. The amplitude of the total spectrum considerably exceeds the amplitude of the TR spectrum from the amorphous layer in the case when the crystal is used only for separation of photons by their frequency (curve $T_{DTR}^{(s)}$). In the case of destructive interference of TR waves from the amorphous layer and the front boundary of the crystal layer, total DTR can be suppressed, which is demonstrated by the curves in Fig. 4. In this case, only the thickness of the vacuum layer of the target has changed as compared to the case depicted in Fig. 3.

In Fig. 5, the curves of the total DTR spectrum are constructed in the case of constructive (parameter $a/b = 2m + 1$) and destructive (parameter $a/b = 2(2m + 1)$) interference of TR waves against the background of PXR. The curve describing the PXR spectrum is plotted in accordance with formula (9b). Although, as noted above, the PXR spectral–angular density is independent of the parameters of the amorphous layer, the term in the expression for the density of resultant radiation, which is the result of interference of PXR and DTR, depends on these parameters. This term in formula (10b) under the specified conditions produces a negligibly small effect on the total radiation spectrum and is not shown in the figure for this reason. It follows from Fig. 5 that by changing the thickness $a$ of the vacuum layer for a fixed thickness $b$ of the crystal layer, it is possible to suppress the DTR spectrum for a given observation angle due to the

destructive interference of TR waves from the amorphous layer and the front boundary of the crystal layer. This effect makes it possible to analyze PXR from thin crystal targets and/or use it in applications (where transition radiation from each surface becomes comparable in amplitude with parametric radiation) in the absence of a DTR background.

Expressions (4) and (9) describing the spectral–angular DTR densities were derived above for the general case of reflection of the electromagnetic field in the crystal layer asymmetric relative to the surface. The asymmetry of reflection is characterized by parameter $\varepsilon$ determining angle $\delta$ between the system of parallel atomic planes in the crystal layer and its surface for a fixed Bragg angle $\theta_B$. It should be noted that for a fixed $\theta_B$, the angle $\delta - \theta_B$ of incidence of an electron on the target surface decreases upon an increase in parameter $\varepsilon$. In the case of symmetric reflection, we have $\varepsilon = 1$ and $\delta = \pi/2$.

Figure 6 shows the curves describing the spectral–angular DTR density for a fixed observation angle $\theta$. The curves demonstrate a substantial increase in the amplitude of the DTR spectrum upon an increase in the asymmetry parameter $\varepsilon$ (the decrease in the angle of incidence $\delta - \theta_B$ of an electron on the target) for a fixed $\theta_B$. Thus, changing the asymmetry of reflection, it is possible to substantially increase the spectral–angular DTR density from the three-layer structure under investigation. With an increase in the parameter $\varepsilon$, the width of the PXR spectrum increases. This parametric effect is associated with the fact that with increasing $\varepsilon$, the dependence of the denominator $\sigma^{(s)} + (\xi - \sqrt{\xi^2 + \varepsilon})/\varepsilon$ in formula (9c) on spectral variable $\eta^{(s)}(\omega)$ becomes weaker. In other words, upon an increase in $\varepsilon$, the departure from resonance $\sigma^{(s)} + (\xi -$
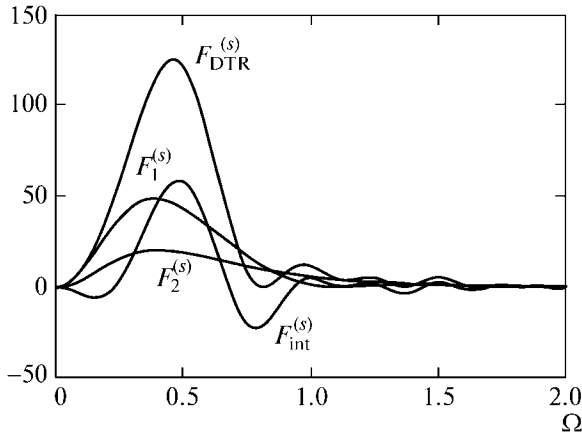
Fig. 8. Contributions $F_1^{(s)}$ of TR waves from amorphous wafer, $F_2^{(s)}$ of TR waves from front boundary of the crystal layer, and $F_{int}^{(s)}$ of interference term to total angular density $F_{DTR}^{(s)}$ of DTR. Curves are plotted for $\Gamma = 0.5$, $\chi_c'/\chi_0' = 0.5$, $B^{(s)} = 5$, $v^{(s)} = 0.8$, $\varepsilon = 5$, $a/b = 2m + 1$, $c/b = 0.5(2n + 1)$ for constructive interference at angular density peak.
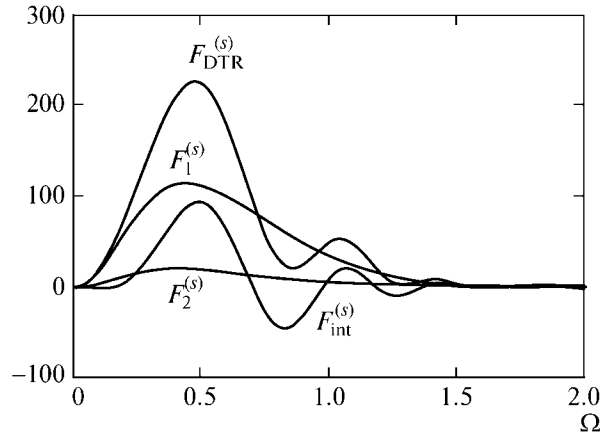


Fig. 9. Same as in Fig. 8, but for parameters $\Gamma = 0.5$, $\chi_c'/\chi_0' = 2$, $B^{(s)} = 5$, $v^{(s)} = 0.8$, $\varepsilon = 5$, $a/b = 2m + 1$, $c/b = 0.2(2n + 1)$ for constructive interference at angular density peak.

$\sqrt{\xi^2 + \varepsilon})/\varepsilon = 0$ in expression (9c) becomes slower. This resonance condition can be used to determine the frequency $\omega$ in the vicinity of which the entire spectrum of PXR photons emitted at a fixed angle of observation $\theta$ is concentrated and which corresponds to the condition of equality of the real parts of the wavevectors of the real and virtual photons (Fig. 7).

Let us consider the angular dependence of radiation. The curves depicted in Fig. 8 are plotted in accordance with formula (12b) and describe the contribution of the TR waves from amorphous wafer (curve $F_{DTR}^{(s)}$), TR waves from the front boundary of the crystal layer (curve $F_1^{(s)}$), and their interference term ($F_{int}^{(s)}$) to the total angular density of DTR $F_2^{(s)}$ (see expression (12c)). The curves are plotted for the same parameters as for the curves in Fig. 3. It can be seen from Fig. 8 that for an increasing angular density of DTR due to constructive interference of TR waves from the amorphous layer and the front boundary of the crystal layer, it is sufficient to ensure the fulfillment of interference conditions at the peak of the DTR angular density, whose position depends on electron energy. Figure 9 shows curves describing the angular dependence of DTR in the case where the density of the material of the amorphous layer (to be more precise, the real part of its dielectric susceptibility) is higher that of the crystal layer ($\chi_c'/\chi_0' = 2$). To preserve the constructive interference conditions for waves from different boundaries of the amorphous layer (see expression (14a)), the curves in Fig. 9 were

plotted for a ratio $c/b$ differing from that in Fig. 8. Figure 9 shows that the contribution of the interference term can be significant even in the case of a small contribution of the TR waves from the front boundary of the crystal layer to the total angular density of DTR. A comparison of the total DTR angular density for different values of ratio $\chi_c'/\chi_0'$ is illustrated in Fig. 10. It can be seen that with an increasing ratio $\chi_a'/\chi_0'$, the total angular density increases substantially. The curves in Fig. 11 demonstrate a strong effect asymmetry (relative to the surface of the crystal layer) of reflec-
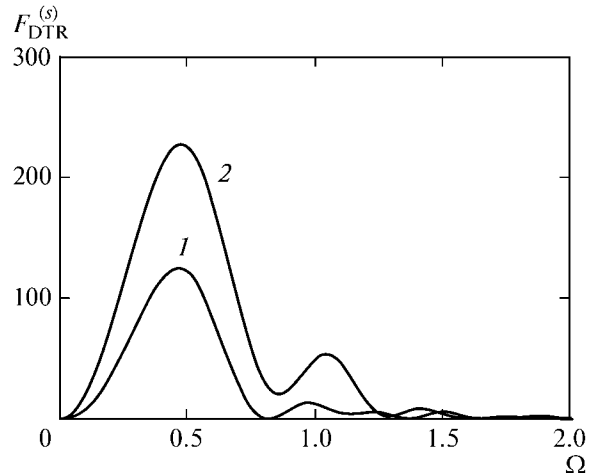


Fig. 10. Angular density of DTR for constructive interference at angular density peak for different ratios $\chi_c'/\chi_0'$: $\Gamma = 0.5$, $B^{(s)} = 5$, $v^{(s)} = 0.8$, $\varepsilon = 5$, $a/b = 1$. Curve 1 is plotted for $\chi_c'/\chi_0' = 0.5$, $c/b = 0.5(2n + 1)$; curve 2 is plotted for $\chi_c'/\chi_0' = 2$ and $c/b = 0.2(2n + 1)$.
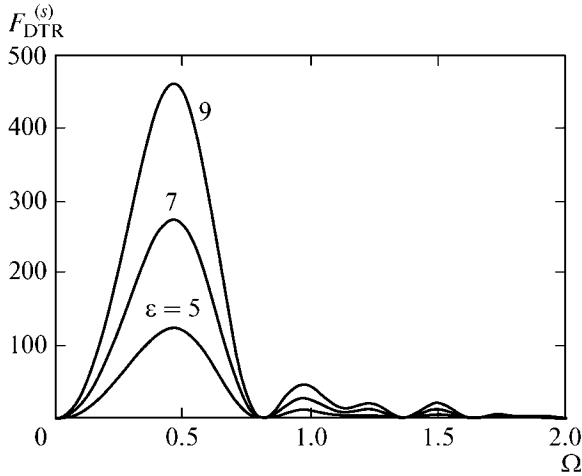
Fig. 11. Effect of asymmetry of reflection in crystal layer on angular density of DTR. Parameters are same as Fig. 8.



Fig. 12. Relative contributions of PXR, DTR, and their interference term to total angular density. Parameters are same as Fig. 8.

tion of the Coulomb field of an electron (parameter $\varepsilon$) on the DTR angular density from the three-layer structure under investigation. The curves in Figs. 12 and 13 were plotted in accordance with formulas (12c), (13b), and (14b) and demonstrate the relative contributions of the angular densities of DTR, PXR, and their interference term to the total angular density. The curves in Fig. 13 were plotted for electron energy twice as high as the energy for which the curves in Fig. 12 were constructed. It can be seen that the DTR angular density at its maximum has thereby increased almost tenfold.

Thus, the expressions derived here make it possible to optimize the spectral–angular characteristics of the coherent X-ray radiation of a relativistic electron crossing the three-layer target under investigation. The possibility of creating a substantial (several-times) increase in the spectral–angular density of DTR in such a target by selecting its parameters paves the way for the application of the three-layer target described here as an emitter of high-intensity monochromatic tunable X-ray source based on diffracted transition radiation of a relativistic electron.

## 5. CONCLUSIONS

We have analyzed the conditions for the coherent addition of transient radiation waves generated by a relativistic electron in a three-layer emitter consisting of two amorphous layers and a single-crystal layer (in particular, the emitter whose second layer is vacuum). We have determined the parameters of the layers and the substances constituting them that are optimal for the selected radiation frequency. The possibility of a ninefold increase in the intensity of the diffracted transition radiation generated by a relativistic electron in such a target is demonstrated.
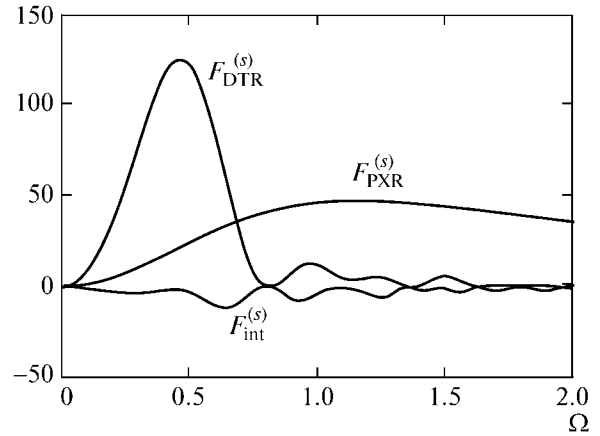
Using the two-wave approximation of the dynamic theory of diffraction of X-ray waves in a crystal, we have derived the expressions describing the spectral and angular characteristics of diffracted transition radiation, parametric X-ray radiation of a relativistic electron in the structure under investigation, and their interference. The possibility of a substantial increase in DTR yield due to the overall contribution of transition radiation from the amorphous layer and the front boundary of the crystal layer in the conditions of constructive interference has been demonstrated. It is shown that in the case of destructive interference of TR waves, there exist the conditions of a complete suppression of DTR in the three-layer structure under investigation, which makes it possible to observe PXR
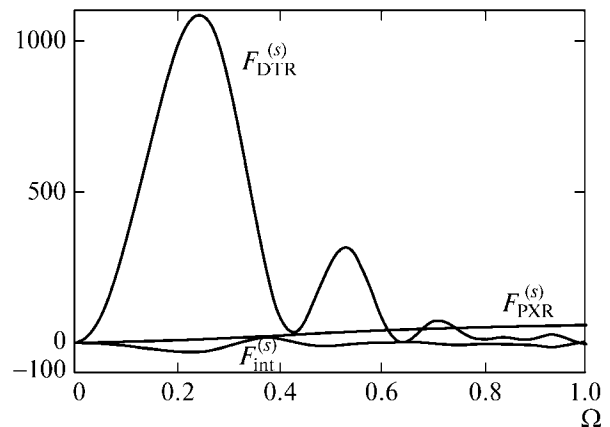


Fig. 13. Relative contributions of PXR, DTR, and their interference term to he total angular density. Energy of emitting electron is twice as high ($\Gamma = 0.25$) as in Fig. 12. Curves are plotted for parameters $\chi_c' / \chi_0' = 0.5$, $B^{(s)} = 5$, $v^{(s)} = 0.8$, $\varepsilon = 5$, $a/b = 4(2m + 1)$, and $c/b = 0.8(2n + 1)$ for constructive interference at angular density peak.

in a thin crystal wafer for which the peaks of the DTR and PXR spectra are hardly distinguishable without a background.

It is shown that asymmetry of reflection of the electron field in the crystal layer considerably affects the spectral and angular characteristics of radiations; the DTR angular density can be increased using a high-density amorphous layer. Our results can be used to design a high-intensity quasi-monochromatic source of X-ray radiation.

## ACKNOWLEDGMENTS

## REFERENCES

1. R. Rullhusen, X. Artru, and P. Dhez, *Novel Radiation Sources Using Relativistic Electrons* (World Scientific, Singapore, 1999).

2. V. L. Ginzburg and I. M. Frank, Zh. Eksp. Teor. Fiz. **16**, 15 (1946).

3. V. L. Ginzburg and V. N. Tsytovich, *Transition Radiation and Transition Scattering* (Nauka, Moscow, 1984; Adam Hilger, Bristol, United Kingdom, 1990).

4. G. M. Garibyan and C. Yang, Sov. Phys. JETP **34** (3), 495 (1971).

5. V. G. Baryshevskii and I. D. Feranchuk, Sov. Phys. JETP **34** (3), 502 (1971).

6. M. A. Kumakhov, Phys. Lett. A **5**, 17 (1976).

7. R. Carr, Nucl. Instrum. Methods. Phys. Res., Sect. B **122**, 625 (1994).

8. A. Caticha, Phys. Rev. A: At., Mol., Opt. Phys. **40**, 4322 (1989).

9. V. Baryshevsky, Nucl. Instrum Methods Phys. Res., Sect. A **122**, 13 (1997).

10. X. Artru and P. Rullhusen, Nucl. Instrum. Methods Phys. Res., Sect. B **145**, 1 (1998).

11. N. Nasonov, Phys. Lett. A **246**, 148 (1998).

12. A. V. Koltsov and A. V. Serov, J. Exp. Theor. Phys. **116** (5), 732 (2013).

13. A. V. Serov and B. M. Bolotovskii, J. Exp. Theor. Phys. **104** (6), 866 (2007).

14. M. I. Ryazanov, J. Exp. Theor. Phys. **98** (3), 478 (2004).

15. A. P. Potylitsyn and R. O. Rezaev, Nucl. Instrum. Methods Phys. Res., Sect. B **252**, 44 (2006).

16. D. Yu. Sergeeva, A. A. Tishchenko, and M. N. Strikhanov, Nucl. Instrum. Methods Phys. Res., Sect. B **309**, 189 (2013).

17. N. F. Shul'ga and V. V. Syshchenko, Nucl. Instrum. Methods Phys. Res., Sect. B **201**, 78 (2003).

18. N. Nasonov, Phys. Lett. A **292**, 146 (2001).

19. N. Nasonov and A. Noskov, Nucl. Instrum. Methods Phys. Res., Sect. B **201**, 67 (2003).

20. S. Blazhevich and A. Noskov, Nucl. Instrum. Methods Phys. Res., Sect. B **252**, 69 (2006).

21. S. V. Blazhevich and A. V. Noskov, Nucl. Instrum. Methods Phys. Res., Sect. B **266**, 3770 (2008).

22. S. V. Blazhevich and A. V. Noskov, J. Exp. Theor. Phys. **109** (6), 901 (2009).

23. S. V. Blazhevich and A. V. Noskov, J. Exp. Theor. Phys. **118** (4), 550 (2014).

24. Z. G. Pinsker, *Dynamical Scattering of X-Rays in Crystals* (Nauka, Moscow, 1974; Springer-Verlag, Berlin, 2012).

25. S. V. Blazhevich, I. V. Kolosova and A. V. Noskov, J. Surf. Invest. **6** (2), 348 (2012).

26. V. A. Bazylev and N. K. Zhevago, *Radiation of Fast Particles in Matter and External Fields* (Nauka, Moscow, 1987) [in Russian].

*Translated by N. Wadhwa*